Journal of Medicinal Chemistry

Subscriber access provided by American Chemical Society

Article

Pyrazolo[3,4-*c*]pyridazines as Novel and Selective Inhibitors of Cyclin-Dependent Kinases

Miguel F. Braa, Mnica Cacho, M. Luisa Garca, Elena P. Mayoral, Berta Lpez, Beatriz de Pascual-Teresa, Ana Ramos, Nuria Acero, Francisco Llinares, Dolores Muoz-Mingarro, Olivier Lozach, and Laurent Meijer

J. Med. Chem., **2005**, 48 (22), 6843-6854• DOI: 10.1021/jm058013g • Publication Date (Web): 08 October 2005

Downloaded from http://pubs.acs.org on March 29, 2009

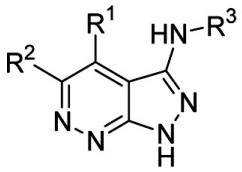

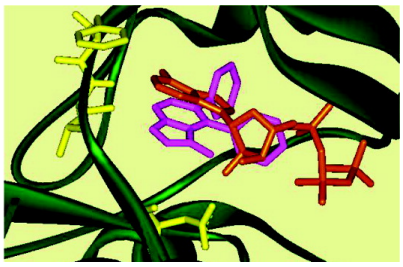

More About This Article

Additional resources and features associated with this article are available within the HTML version:

- Supporting Information
- Links to the 6 articles that cite this article, as of the time of this article download
- Access to high resolution figures
- Links to articles and content related to this article
- Copyright permission to reproduce figures and/or text from this article

View the Full Text HTML

ACS Publications
High quality. High impact.

Journal of Medicinal Chemistry is published by the American Chemical Society. 1155 Sixteenth Street N.W., Washington, DC 20036

Pyrazolo[3,4-*c*]pyridazines as Novel and Selective Inhibitors of Cyclin-Dependent Kinases

Miguel F. Braña,*,† Mónica Cacho,† M. Luisa García,† Elena P. Mayoral,† Berta López,† Beatriz de Pascual-Teresa,† Ana Ramos,† Nuria Acero,# Francisco Llinares,§ Dolores Muñoz-Mingarro,† Olivier Lozach,‡ and Laurent Meijer‡

Facultad de Farmacia, Universidad San Pablo CEU, Urbanización Montepríncipe, 28668-Boadilla del Monte, Madrid, Spain, and CNRS, Cell Cycle Group, UPS 2682 & UMR 2775, Station Biologique, B.P. 74, 29682 Roscoff Cedex, Bretagne, France

Received March 1, 2005

Pyrazolopyridazine **1a** was identified in a high-throughput screening carried out by BASF Bioresearch Corp. (Worcester, MA) as a potent inhibitor of CDK1/cyclin B and shown to have selectivity for the CDK family. Analogues of the lead compound have been synthesized and their antitumor activities have been tested. A molecular model of the complex between the lead compound and the CDK2 ATP binding site has been built using a combination of conformational search and automated docking techniques. The stability of the resulting complex has been assessed by molecular dynamics simulations and the experimental results obtained for the synthesized analogues have been rationalized on the basis of the proposed binding mode for compound **1a**. As a result of the SAR study, monofuryl **1o** has been synthesized and is one of the most active compounds against CDK1 of this series.

Introduction

Cyclin-dependent kinases (CDKs) are a family of serine/threonine kinases that regulate the cell division cycle phases, apoptosis, transcription, and differentiation in addition to other functions in the nervous system.[1] Each CDK associates with a specific cyclin regulatory partner to generate the active catalytic complex. Owing to both their central role in the cell cycle and their misregulation in a number of cancers[2] and neurodegenerative disorders, CDK inhibitors have garnered attention recently for their potential as anticancer therapeutics.[1,3,4]

The search for small-molecule inhibitors of CDKs has already led to the discovery of several classes of compounds with high structural diversity.[1,3,4] Only reports on the clinical trial of flavopiridol and UCN-01 as cancer therapeutics are available,[5−7] but several other CDK inhibitors are currently making their way in the clinic. Despite striking chemical diversity, most CDK inhibitors share common properties. Thus, they are essentially low molecular weight, flat, hydrophobic heterocycles and act by competing with ATP for binding in the kinase ATP binding site.

Pyrazolopyridazine **1a** was identified in a high-throughput screening carried out by BASF Bioresearch Corp. (Worcester, MA) as a potent inhibitor of CDK1/cyclin B. Subsequent screening of this hit against other kinases revealed the compound to have selectivity for the CDK family (IC_{50} (μM) for different kinases: CDK1/cyclin B = 6.1, kdr > 50, and lck > 50). This prompted us to synthesize a new series of pyrazolo[3,4-*c*]pyridazine analogues of **1a** in an attempt to improve potency against the CDK family while maintaining a favorable selectivity profile and to carry out a structure−activity relationship study. The emphasis has been put on the molecular modulation. Specifically, (a) different substituents in the aromatic system at C-4 and C-5 have been introduced, (b) phenyl rings have been substituted by other groups, (c) the amino group at the C-3 position has been substituted by other functions, and (d) different substituents have been introduced at position 1 (Figure 1).

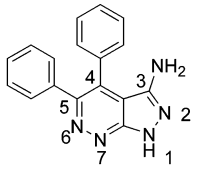

1a

CDK1/cyclin B: IC_{50} = 6.1 μM
kdr: IC_{50} > 50 μM
lck: IC_{50} > 50 μM

While this work was in progress, Witherington et al.[8] have also identified pyrazolopyridazine **1a** as a potent inhibitor of glycogen synthase kinase-3 (GSK-3) and CDK2/cyclin A. In this work, this compound also showed excellent selectivity against the majority of the tested kinases. This result is not unexpected given the high homology between these two kinases and CDK1. GSK-3 has a major role in the regulation of the cell cycle, transcription, and insulin action. As in the case of CDKs, this type of kinase is involved in cancer and neurodegenerative diseases and it has also been used as a target to identify small molecular weight pharmacological inhibitors of potential therapeutic interest. Therefore, inhibitors that show dual specificity for these kinases could be useful in the treatment of cancer.[1,9]

* To whom the correspondence should be addressed. Phone: 34913724700. Fax: 34913510475. E-mail: mfbrana@ceu.es.
† Departamento de Química, Universidad San Pablo CEU.
# Departamento de Ciencias Ambientales y Recursos Naturales, Universidad San Pablo CEU.
§ Departamento de Biología Celular, Bioquímica y Biología Molecular, Universidad San Pablo CEU.
‡ CNRS, Cell Cycle Group.

10.1021/jm058013g CCC: $30.25 © 2005 American Chemical Society
Published on Web 10/08/2005

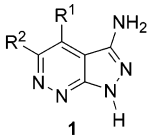

1

1a: $R^1 = R^2 = C_6H_5$
1b: $R^1 = R^2 = p\text{-}C_6H_5C_6H_4$
1c: $R^1 = R^2 = p\text{-}NO_2C_6H_4$
1d: $R^1 = R^2 = p\text{-}{}^t\text{Bu}C_6H_4$
1e: $R^1 = R^2 = p\text{-}CF_3C_6H_4$
1f: $R^1 = R^2 = p\text{-}CH_3OC_6H_4$
1g: $R^1 = R^2 = 2,2'$-biphenyl
1h: $R^1 = R^2 = 2$-furyl
1i: $R^1 = R^2 = 2$-pyridyl
1j: $R^1 = R^2 = CH_3$
1k: $R^1 = C_6H_5$; $R^2 = CH_3$
1l: $R^1 = C_6H_5$; $R^2 = H$
1m: $R^1 = R^2 = p\text{-}NH_2C_6H_4$
1n: $R^1 = H$; $R^2 = C_6H_5$
1o: $R^1 = H$; $R^2 = 2$-furyl

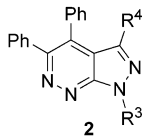

2

2a: $R^3 = H$; $R^4 = OH$
2b: $R^3 = H$; $R^4 = NHCONHEt$
2c: $R^3 = H$; $R^4 = NHCONHC_6H_5$
2d: $R^3 = H$; $R^4 = NHNH_2$
2e: $R^3 = H$; $R^4 = NHCOCH_3$
2f: $R^3 = COCH_3$; $R^4 = NH_2$
2g: $R^3 = COCH_3$; $R^4 = NHCOCH_3$
2h: $R^3 = CH_2C_6H_5$; $R^4 = NH_2$
2i: $R^3 = CH_2O(CH_2)_2OH$; $R^4 = NH_2$
2j: $R^3 = (CH_2)_2O(CH_2)_2OH$; $R^4 = NH_2$

Figure 1. Structures of pyrazolopyridazine-based CDK1 inhibitors.

Scheme 1[a]

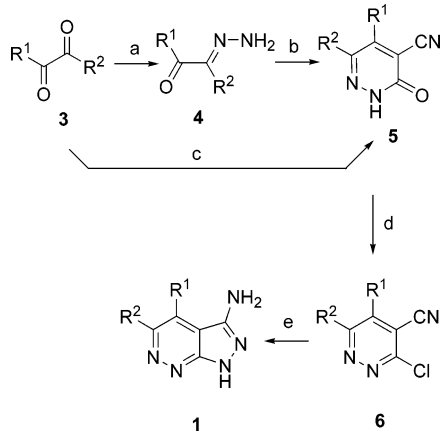

[a] Reagents: (a) NH_2NH_2, EtOH, Δ; (b) (i) Na, EtOH, ethyl cyanoacetate; (ii) 1 N HCl; (c) cyanoacetohydrazide, EtOH, or DMF, Δ; (d) $POCl_3$, dioxane, Δ; (e) NH_2NH_2, EtOH, Δ.

Results and Discussion

Chemistry. The method utilized for the synthesis of pyrazolo[3,4-*c*]pyridazines **1a**−**l** is outlined in Scheme 1. The necessary 1,2-dicarbonyl compounds were commercially available (**3a** and **3f**−**l**) or easily prepared (**3b**−**d**) following previously described methods.[10−12] Diketone **3e** was described as a secondary product (10%) in the synthesis of ethyl 2-oxo-2-(*p*-trifluoromethylphenyl)acetate, by reaction of trifluoromethylphenyl bromide with diethyl oxalate in the presence of BuLi.[13] We have found that with the use of equivalent amounts of reactants and a high excess of base, the yield of the desired diketone can be increased to 25%.

Scheme 2[a]

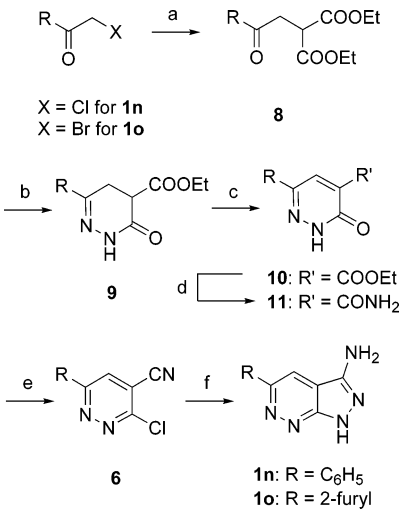

[a] Reagents: (a) diethyl malonate, K_2CO_3, KI; (b) NH_2NH_2, EtOH; (c) Br_2, AcOH; (d) NH_3; (e) $POCl_3$, dioxane, Δ; (f) NH_2NH_2, EtOH.

The desired pyridazinones have been obtained following two alternative methods. Compounds **5d**−**f** were obtained by reaction of diketones **3d**−**f** with an excess of hydrazine in EtOH, followed by reaction of the corresponding monohydrazones **4d**−**f** with ethyl cyanoacetate and NaOEt. On the other hand, pyridazinones **5a**−**c** and **5g**−**l** were obtained with better yields by reacting the corresponding 1,2-dicarbonyl compounds with cyanoacetohydrazide. The reaction mixture was refluxed in EtOH or DMF except for pyridazinone **5l**, where the condensation between **3l** and cyanoacetohydrazide was performed at room temperature to isolate intermediate **7**, which was then transformed into **5l** by

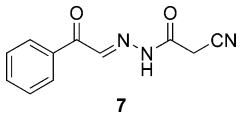

7

treatment with sodium in EtOH. When diketone **3i** was refluxed with cyanoacetohydrazide in EtOH, two compounds were isolated. One of them was the expected reaction product **5i**, and the other was characterized as pyrazolopyridazine **1i**. This result is difficult to explain, unless some amount of hydrazine was present in the reaction medium from partial hydrolysis of cyanoacetohydrazide.

Compounds **5a**−**h** and **5j**−**l** were transformed into the corresponding pyridazines **6a**−**h** and **6j**−**l** by treatment with phosphorus oxychloride. Reaction of these pyridazines with hydrazine yielded the desired pyrazolopyridazines **1a**−**h** and **1j**−**l**.

Compounds **1n** and **1o** were obtained following the method outlined in Scheme 2. Thus, condensation of the corresponding phenacyl halide with diethyl malonate, gave diester **8**, which by reaction with hydrazine followed by oxidation with bromine in AcOH gave compound **10**. Treatment of ester **10** with aqueous ammonia

Scheme 3[a]

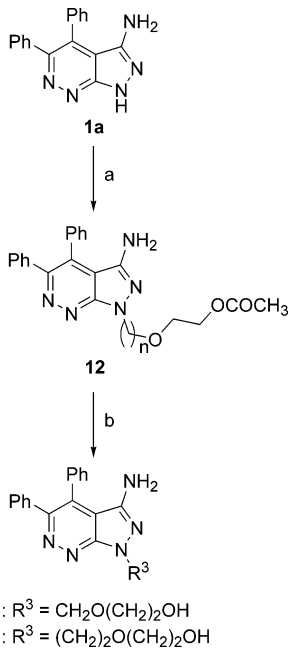

2i: $R^3 = CH_2O(CH_2)_2OH$
2j: $R^3 = (CH_2)_2O(CH_2)_2OH$

[a] Reagents: (a) $X(CH_2)_nO(CH_2)_2OCOCH_3$, X = Br for **2i** and X = I for **2j**, Cs_2CO_3, DMF; (b) 1 N NH_4OH.

at room temperature afforded amide **11**. Subsequent treatment with phosphorus oxychloride in dioxane at reflux temperature afforded chloronitrile **6**. Finally, treatment of **6** with hydrazine gave the desired pyrazolopyridazines **1n** and **1o**. Pyrazolopyridazine **1m** was obtained by reduction of **1c** with Raney Ni and hydrazine.

Pyrazolopyridazine **2a** was obtained by a method similar to that outlined in Scheme 1 but using ethyl 3-hydrazino-3-oxopropionate instead of cyanoacetohydrazide, as described in the literature.[14]

The reaction of **1a** with ethyl isocyanate or phenyl isocyanate yielded compounds **2b** and **2c**, respectively. Similarly, compounds **13** and **14** were obtained from **1o**. Hydrazine **2d** was synthesized by reaction of **1a** with $NaNO_2$/HCl followed by reduction of the formed diazonium salt with Na_2SO_3.

Derivative **2e** was obtained by refluxing **1a** with acetyl chloride and Et_3N in dioxane. Under these conditions, acetylation took place selectively at the amino group in the 3 position. However, when the reaction was carried out by heating the reactants in the presence of pyridine, compound **2f** was isolated. Diacetylation was observed when **1a** was treated with acetic anhydride in AcOH, yielding compound **2g**.

Pyrazolopyridazine **2h** was synthesized by reaction of **6a** with phenylhydrazine. Finally, compounds **2i** and **2j** were obtained by reaction of **1a** with the corresponding halogeno derivative in the presence of Cs_2CO_3, followed by hydrolysis of the ester group present in **12** with 1 N NH_4OH, as depicted in Scheme 3.

Biological Activity. Compounds **1** were tested for their ability to inhibit in vitro the CDK1/cyclin B complex from starfish (*Marthasterias glacialis*) oocytes as described Meijer et al.[15] In this assay the transfer of γ-^{33}P-labeled phosphate from [γ-^{33}P]ATP to histone H1 in the absence and presence of inhibitor is measured and expressed as a percent of kinase activity without inhibitor. The IC_{50} is determined from dose response curves. The IC_{50} value for each of the compounds determined under these assay conditions is shown in Tables 1 and 2.

We also tested the synthesized compounds for their cytotoxic effects against several cancer cell lines. These include human colon carcinoma (HT-29), human cervical carcinoma (HeLa), and human prostate carcinoma (PC-3), and the results are presented in Tables 1 and 2.

To investigate the effect of substitution on the aromatic rings, a small number of compounds (**1b**−**f** and **1m**) were synthesized and their potency in the purified enzyme assay was measured. Compounds **1c** and **1e**, bearing electron-withdrawing groups in the para position of both aromatic rings, were found to be inactive against CDK1/cyclin B and all the cell lines tested. In contrast, compound **1f**, where a donor group is present in the same position, was able to inhibit the enzyme, although a 5-fold drop in potency was found, compared to the lead compound **1a**.

The proposed binding mode for compound **1a** (see later) suggests that the aromatic ring in position 5 may display van der Waals interactions with vicinal amino acid residues in the enzyme. On the basis of this model, it was anticipated that derivatives **1b** and **1d**, where the aromatic rings bear a bulky substituent (phenyl for **1b** and *tert*-butyl for **1d**), would be significantly weaker inhibitors of CDK1. Indeed, both of them failed to inhibit CDK1 at all concentrations up to 50 μM.

Replacement of the aromatic rings in positions 4 and 5 of the pyrazolopyridazine system in **1a** by a π-rich furan ring (**1h**) led to a potent CDK1/cyclin B inhibitor (IC_{50} = 1.5 μM), while an inactive compound (**1i**) was obtained when a π-deficient ring was introduced. From an electrostatic point of view, this result is in accordance with the previous observation that electron-rich aromatic rings in positions 4 and 5 have a favorable effect on the inhibitory activity. The anti-CDK1 activity of **1h** was not accompanied by antitumor activity in the cell lines tested.

The next modifications of **1a** to be examined were the elimination of one of the aromatic rings in positions 4 and 5 (**1l** and **1n**) and the substitution of one or both of the aromatic rings by methyl groups (**1j** and **1k**). Interestingly, only compound **1n** maintained the activity of the lead compound against the enzyme. This finding suggested that the presence of an aromatic ring in position 5 of compound **1a** is essential for its inhibitory activity. However, the aromatic ring in position 4 can be eliminated without resulting in a loss of activity. Again, the molecular modeling study gave us a possible explanation for this behavior. According to the proposed binding mode for compound **1a**, which will be discussed later, the aromatic ring in position 5 is located in a hydrophobic pocket formed by residues Val18, Ala31, Val64, Phe80, and Ala144, while the aromatic ring in position 4 does not establish any relevant interaction.

Pyrazolopyridazine **1g**, where the connection of both phenyl groups by means of a cyclohexane ring rigidified the system, did not present inhibitory activity. This result is also in accordance with the proposed binding mode (Figure 2), where the phenyl groups in **1a** are oriented in a parallel disposition. Obviously, the rigidification carried out in compound **1g** does not allow the

Table 1. Enzymatic and Cellular Activity for Compounds **1**

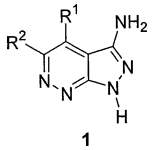

1

compd	R^1	R^2	HT-29[a] IC_{50}, μM	HeLa[b] IC_{50}, μM	PC-3[c] IC_{50}, μM	CDK1/cyclin B IC_{50}, μM
1a	C_6H_5	C_6H_5	>100	>100	>100	3.00
1b	*p*-$C_6H_5C_6H_4$	*p*-$C_6H_5C_6H_4$	>100	>100	NT	>50
1c	*p*-$NO_2C_6H_4$	*p*-$NO_2C_6H_4$	>100	>100	NT	>50
1d	*p*-^{t}BuC_6H_4	*p*-^{t}BuC_6H_4	8.50	8.78	NT	>50
1e	*p*-$CF_3C_6H_4$	*p*-$CF_3C_6H_4$	>100	>100	NT	>50
1f	*p*-$CH_3OC_6H_4$	*p*-$CH_3OC_6H_4$	>100	>100	>100	15.00
1g	2,2′-biphenyl	2,2′-biphenyl	>100	30.70	>100	>50
1h	2-furyl	2-furyl	>100	>100	NT	1.50
1i	2-pyridyl	2-pyridyl	73.00	>100	NT	>50
1j	CH_3	CH_3	>100	>100	NT	>50
1k	C_6H_5	CH_3	>100	88.30	72.40	>50
1l	C_6H_5	H	80.80	>100	NT	>50
1m	*p*-$NH_2C_6H_4$	*p*-$NH_2C_6H_4$	10.52	>100	NT	>50
1n	H	C_6H_5	>100	>100	NT	4.00
1o	H	2-furyl	>100	>100	>100	5.30
flavopiridol						0.4[d]
olomoucine						7[d]
purvalanol B						0.006[d]

[a] Human colon carcinoma cell line. [b] Human cervical carcinoma cell line. [c] Human prostate carcinoma cell line. [d] From literature.[4]

Table 2. Enzymatic and Cellular Activity for Compounds **2**

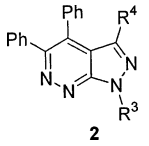

2

compd	R^3	R^4	HT-29 IC_{50}, μM	HeLa IC_{50}, μM	PC-3 IC_{50}, μM	CDK1/cyclin B IC_{50}, μM
2a	H	OH	>100	>100	>100	>50
2b	H	NHCONHEt	>100	60.44	>100	7.50
2c	H	$NHCONHC_6H_5$	>100	2.93	>100	9.00
2d	H	$NHNH_2$	NT	NT	NT	8.50
2e	H	$NHCOCH_3$	>100	>100	>100	>50
2f	$COCH_3$	NH_2	>100	>100	>100	>50
2g	$COCH_3$	$NHCOCH_3$	>100	>100	>100	>50
2h	$CH_2C_6H_5$	NH_2	>100	>100	>100	>50
2i	$CH_2O(CH_2)_2OH$	NH_2	>100	>100	>100	>50
2j	$(CH_2)_2O(CH_2)_2OH$	NH_2	>100	>100	>100	>50

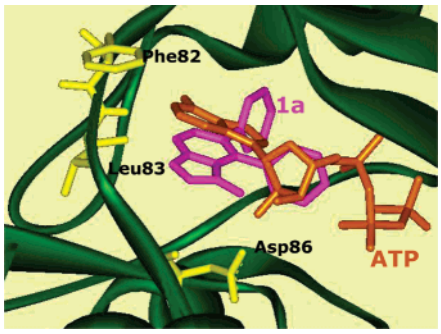

Figure 2. Binding model of **1a** and ATP in the CDK2 active site. Residues relevant to the discussion are displayed as thick sticks in yellow.

molecule to adopt that orientation of the phenyl groups in the binding site.

Pyrazolopyridazines having more lipophilic substituents at C-3 such as acetamide **2e** did lead to a loss of activity. By contrast, the use of other groups capable of establishing additional hydrogen bonds with the enzyme, such as ureas **2b** and **2c** and hydrazine **2d**, maintained the inhibitory activity. Surprisingly, compound **2a**, with a hydroxyl group in the same position, proved to be inactive, while the theoretical work described later predicts a very similar orientation of compounds **1a** and **2a** inside the binding pocket of CDK2.

Finally, compounds **2f**–**j** were designed to evaluate the effect of substitution in position 1 of the lead compound. Hydroxyethoxymethyl and hydroxyethoxyethyl groups present in **2i** and **2j**, respectively, were chosen because these fragments are present in some antiviral agents, such as aciclovir,[16] a nucleoside analogue inhibitor of the herpex simplex virus. In aciclovir, these groups mimic the carbohydrate fragment present in nucleosides. Our CDKs inhibitors were designed to occupy the ATP binding site in CDK1. Therefore, the presence of hydroxylated chains mimicking the carbohydrate fragment of ATP could increase the affinity and selectivity of the inhibitor. Unfortunately, none of derivatives (**2f**–**j**) exhibited CDK1 inhibitory or antitumor activity, demonstrating that position 1 in the

pyrazolopyridazine system must be unsubstituted for CDK1 inhibition. This result is also in agreement with the modeling work carried out for these compounds and is described below, since the introduction of substituents in position 1 would prevent the electrostatic interaction with Phe82.

Taking into account that the most active compound tested so far is pyrazolopyridazine **1h** and that substitution at position 4 is not essential for activity, the next step in our SAR study was the synthesis and biological evaluation of the monofuryl **1o** and their urea and thiourea derivatives **13** and **14**, respectively. Com-

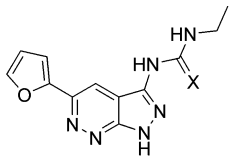

13: X = O CDK1/cyclin B: IC_{50} = 8.8 μM
14: X = S CDK1/cyclin B: IC_{50} > 100 μM

pounds **1o** and **13** were active against CDK1 as we had expected. More interestingly, these two compounds were also active against GSK-3 with IC_{50} values of 0.80 and 0.66 μM, respectively, which enhances their potential utility in the treatment of tumoral affections.

Disappointingly, the synthesized compounds did not show cytotoxic effects against the cell lines tested. This fact could be attributed to their difficulty in crossing cell membranes, even though these compounds fit the broad Lipinski guidelines, and validation of this argument will have to await the results of additional studies.

Molecular Modeling. We have carried out a molecular modeling study on the mode of interaction of compound **1a** with CDK2, making use of automated docking methods and molecular dynamics simulations. Although the inhibitory activity has been tested against CDK1, these studies have been carried out with CDK2 because only X-ray structures of CDK2 in complex with small-molecule ligands have been solved to date, which limits the structure-based studies to this cyclin-dependent kinase. However, the two protein kinases have nearly 66% sequence identity overall, and their ATP binding pockets are quite similar.[17] This issue is extensively explored in a recent work carried out by McGrawth et al., where a homology model of CDK1/cyclinB is generated from a high-resolution CDK2/cyclin A crystal structure.[18] It is therefore possible to assume that these compounds will not show selectivity between these two kinases. We and other authors have previously made use of this approximation in similar studies.

First, the ligand was submitted to a Monte Carlo conformational search, and then the lowest energy conformation was taken as the starting conformation for the automated docking into CDK2. The lowest energy complex predicted by AutoDock is shown in Figure 2. As shown in this figure, compound **1a** binds to the active site of CDK2, with the pyrazolopyridazine system in a position similar to that of the purine ring of the ATP molecule, which is the natural substrate of the enzyme but in a different orientation. Compound **1a** establishes hydrogen bonds with Asp86 and Leu83, residues that are also involved in interactions with the ATP molecule, as shown schematically in Figure 3. In

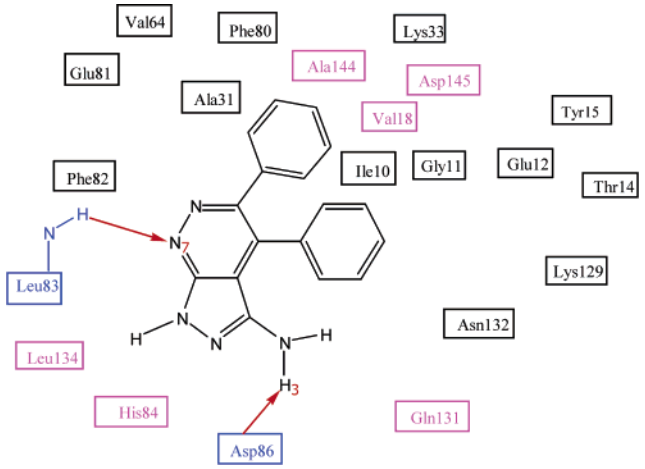

Figure 3. Schematic representation of the binding mode of compound **1a** to CDK2, showing residues with which the ligand interacts through hydrogen bonds (blue) or through van der Waals interactions (magenta).

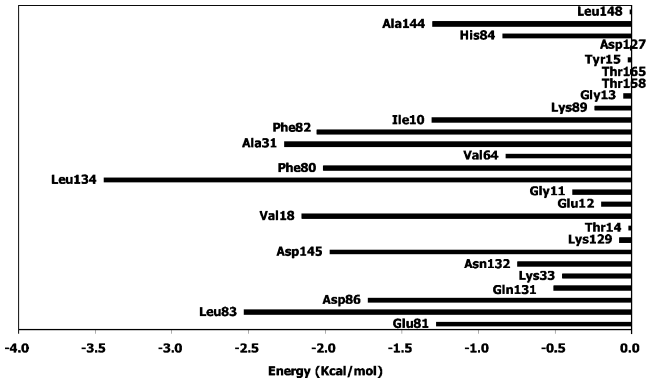

Figure 4. Residue-based van der Waals energy term (kcal/mol) of the interaction between compound **1a** and the CDK2 active site.

the proposed binding mode predicted by AutoDock, residues Val18, Ala31, Val64, Phe80, and Ala144 form a hydrophobic pocket where the phenyl ring in position 5 remains allocated, while the phenyl ring in position 4 does not establish any relevant interaction.

The evidence that proteins that constitute therapeutic targets are mobile is substantial.[19] To take into account protein flexibility, the behavior of the predicted complex was studied in a dynamic context and the progression of the root-mean-square (rms) deviation of the coordinates of the solute with respect to the initial structure was monitored, leading to an average value of 3.186 ± 0.623 Å. The progression of this parameter indicates that the complex does not experience large conformational changes during the sampling time and, thus, can be considered to be in a state near equilibrium. To evaluate the relative contributions of the different residues to complex stabilization, the 125 structures collected from the last 500 ps of the simulation were averaged and energy-minimized, and the interaction energy between compound **1a** and the binding site was decomposed on a residue basis using the ANAL module of AMBER (Figures 4 and 5). A superimposition of the energy-minimized average structure and the initial structure is shown in Figure 6. As expected from the calculated rms deviations mentioned above, the complex remains stable along the simulation time; thus, the conformational changes are not very relevant. The

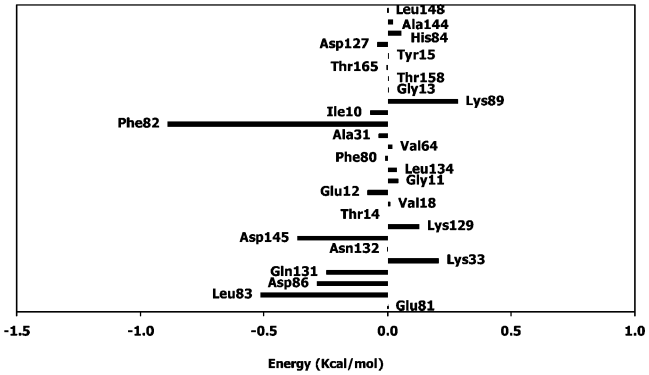

Figure 5. Residue-based electrostatic energy term (kcal/mol) of the interaction between compound **1a** and the CDK2 active site.

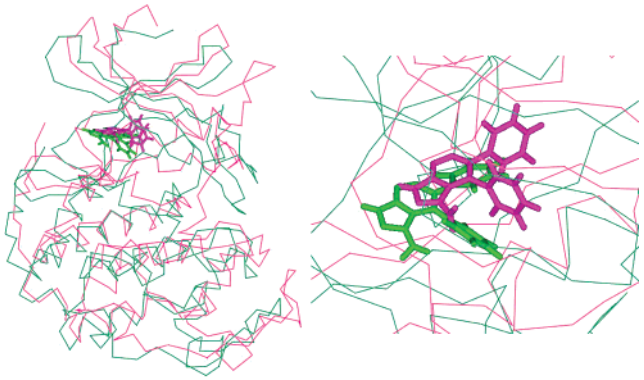

Figure 6. View of superimposed C(α) traces of the energy-minimized average structure of the last 500 ps of the MD simulation (green) and the initial structure (magenta) for CDK2/**1a**.

model we propose for the **1a**/CDK2 complex gives rise to rather strong electrostatic interactions with Phe82, Leu83, Asp86, Gln131, and Asp145.

Leu83 and Asp86 are involved in the formation of two stable hydrogen bonds with positions 7 and 3 from the ligand, respectively. These distances were monitored along the simulation time, demonstrating the stability of the above-mentioned interactions. These interactions seem to be especially relevant for the binding affinity and selectivity of the ligand, since they have also been found to interact with other known CDK inhibitors such as purvalanol B and staurosporine.[3]

On the other hand, Phe82 establishes a strong electrostatic interaction with the NH in position 1 of the ligand. It can also be seen that the major contributors to the van der Waals energy term are Ile10, Val18, Ala31, Phe80, Glu81, Phe82, Leu83, Asp86, Gln131, Leu134, Ala144, and Asp145.

A similar docking procedure was used to explore the possible binding modes of the synthesized analogues (**1b**−**o** and **2a**−**c**,**e**,**f**). First, the ligands were submitted to a Monte Carlo conformational search, and then the lowest energy conformations were taken as the starting structures for the automated docking into CDK2. This study reveals that all the synthesized compounds interact with the ATP binding pocket of the kinase. However, the binding modes predicted by AutoDock differ significantly from that described above for the lead compound, with the exception of compound **2a**, which adopts a similar orientation. As mentioned before, this result does not match the lack of biological activity demonstrated for this compound. A possible explanation for this unexpected result may be that compound **2a** could be interacting with the enzyme through the 4,5-diphenyl-1,2-dihydropyrazolo[3,4-*c*]pyridazin-3-one tautomeric form (**2a**$_1$). A RHF/6-31G* geometry optimization of the two tautomers led to a 3.8 kcal/mol energy difference in favor of the 4,5-diphenyl-1*H*-pyrazolo[3,4-*c*]pyridazin-3-ol form (**2a**$_2$). However, taking into account that the solvent effect was not considered, we cannot discard the possibility that compound **2a** may be interacting with the enzyme's binding site through the **2a**$_1$ tautomeric form, leading to a completely different binding mode if compared to **1a** and accounting for the lack of activity of the synthesized derivative **2a**.

Conclusions

We have presented a novel series of pyrazolopyridazine-based CDK1 inhibitors. Our SAR study with these compounds suggest that (i) the phenyl rings can be substituted by π-rich rings, such as furan, resulting in a 2-fold increase of inhibition, (ii) substitution at position 4 is not relevant, while the presence of a substituent at position 5 is essential for the potency of CDK1 inhibition, (iii) the introduction of substituents at N-1 led to a loss of activity, (iv) ethylurea, phenylurea, and hydrazine moieties in N-3 maintained the potency of inhibition.

Molecular modeling studies indicate that these molecules create an interaction pattern analogous to that found in many other known small-molecule CDK inhibitors for which structural information is available. According to the proposed binding mode, **1a** binds to the active site of CDK2, with the pyrazolopyridazine system in a position similar to that of the purine ring of the ATP molecule, which is the natural substrate of the enzyme but adopting a different orientation. The proposed binding model for compound **1a** has allowed us to rationalize the CDK1 inhibitory activity observed for the synthesized analogous derivatives.

Experimental Section

General Methods. Melting points (uncorrected) were determined on a Stuart Scientific SMP3 apparatus. Infrared (IR) spectra were recorded with a Perkin-Elmer 1330 infrared spectrophotometer. ^{1}H and ^{13}C NMR δ values were recorded on a Bruker 300-AC instrument. Chemical shifts (δ) are expressed in parts per million relative to internal tetramethylsilane; coupling constants (J) are in hertz. Mass spectra were run on a HP 5989A spectrometer. Elemental analyses (C, H, N) were performed on a Perkin-Elmer 2400 CHN apparatus at the Microanalyses Service of the University Complutense of Madrid. Unless otherwise stated, all reported values are within ±0.4% of the theoretical compositions. Thin-layer chromatography (TLC) was run on Merck silica gel 60 F-254 plates. Unless stated otherwise, starting materials used were high-grade commercial products. The following products were prepared according to the literature: 3-amino-4,5-diphenyl-1*H*-pyrazolo[3,4-*c*]pyridazine **1a**,[20] 3-amino-4,5-dimethyl-1*H*-pyrazolo[3,4-*c*]pyridazine **1j**,[21] 4,5-diphenyl-1*H*-pyrazolo[3,4-*c*]pyridazin-3-ol **2a**.[14] Complete ^{1}H and ^{13}C NMR, IR, MS, and elemental analysis data are given in the Supporting Information.

4,4′-Bis(trifluoromethyl)benzil (3e). A solution of 13.00 mmol of 1.60 M *n*-butyllithium in hexane (8.1 mL) was cooled to −60 °C, and a solution of 2.86 g (13.00 mmol) of 1-bromo-4-trifluoromethylbenzene in 25 mL of anhydride Et_2O was added dropwise. The reaction mixture was warmed to room

temperature and then added dropwise to a solution of 2.85 g (19.55 mmol) of diethyl oxalate in 20 mL of anhydride Et_2O cooled to −60 °C. The reaction mixture was warmed to room temperature, and then the organic layer was washed with 20 mL of water and 10 mL of 2% HCl successively. The combined extracts were dried over $MgSO_4$ and concentrated to give a solid, which was purified by flash chromatography (hexane/Et_2O 98:2) to give **3e**[13] (550 mg, 25%) as a yellow solid. IR (KBr): 1670 cm^{-1}. ^1H NMR ($CDCl_3$): δ 8.01 (4H, d, J = 7.8, ArH), 8.22 (4H, d, J = 7.8, ArH). Further elution afforded 768 mg (24%) of ethyl 2-oxo-2-(*p*-trifluoromethylphenyl)acetate.[13]

2-Cyano-*N*′-(2-oxo-2-phenylethylidene)acetohydrazide (7). To a solution of phenylglyoxal (3.0 g, 22.39 mmol) in 35 mL of absolute EtOH was added 2.22 g (22.39 mmol) of cyanoacetohydrazide at 0 °C. The mixture was stirred for 24 h at room temperature. The precipitated solid was filtered and washed with AcOEt. The combined filtrates were concentrated under reduced pressure to give **7** as a brown oil, which was used without further purification. ^1H NMR (DMSO-d_6): δ 4.19 (2H, s, CH_2), 7.55 (2H, dd, J = 7.3, 7.6, ArH), 7.67 (1H, t, J = 7.3, ArH), 7.79 (1H, s, CH), 8.04 (2H, d, J = 7.3, ArH), 12.30 (1H, sa, NH).

Diethyl 2-[2-(2-Furyl)-2-oxoethyl]malonate (8o). A solution of 320 mg (2.0 mmol) of diethyl malonate, 387 mg (2.0 mmol) of 2-bromo-1-(2-furyl)ethanone,[22] 71 mg (0.43 mmol) of potassium iodide, and 650 mg (4.7 mmol) of potassium carbonate in 30 mL of anhydride acetone was stirred for 24 h at room temperature. After this time, the solvent was eliminated under reduced pressure and the crude of reaction was neutralizated (1 N HCl). The residue was extracted with $CHCl_3$, and the collected organic layers were dried over $MgSO_4$ and concentrated to give a liquid, which was purified by flash chromatography (hexane/AcOEt 7:3) to give **8o** (339 mg, 63%) as a colorless liquid. IR (film): 1670, 1720, 1740 cm^{-1}. ^1H NMR ($CDCl_3$): δ 1.28 (6H, t, J = 7.1, CH_3), 3.49 (2H, d, J = 7.1, CH_2), 4.03 (1H, t, J = 7.1, CH), 4.24 (4H, q, J = 7.1, CH_2), 6.56 (1H, m, furylH), 7.25 (1H, m, furylH), 7.61 (1H, s, furylH). ^{13}C NMR ($CDCl_3$): δ 13.7, 37.0, 46.4, 61.5, 112.1, 117.3, 146.5, 151.7, 168.5, 185.2.

General Procedure for the Preparation of Monohydrazones. A suspension of the corresponding diketone in absolute EtOH containing an excess of $NH_2NH_2{\cdot}H_2O$ was heated at reflux temperature until the reaction was completed (TLC). After the solution was cooled, the formed solid was isolated by filtration and purified by recrystallization from the appropriate solvent or by column chromatography using the appropriate eluents.

Monohydrazone of 4,4′-Di-*tert*-butylbenzil (4d). From 4,4′-di-*tert*-butylbenzil[23] (1.84 g, 5.70 mmol) and $NH_2NH_2{\cdot}H_2O$ (285 mg, 5.70 mmol) in absolute EtOH (30 mL) was obtained **4d** (1.48 g, 77%) as a white solid, mp >300 °C (absolute EtOH). IR (KBr): 1620, 3260, 3390 cm^{-1}. ^1H NMR ($CDCl_3$): δ 1.35 (18H, s, $6CH_3$), 6.25 (2H, sa, NH_2), 7.29 (2H, d, J = 8.8, ArH), 7.47 (2H, d, J = 8.8, ArH), 7.54 (2H, d, J = 8.3, ArH), 7.92 (2H, d, J = 8.3, ArH). ^{13}C NMR ($CDCl_3$): δ 31.1, 31.2, 34.8, 34.9, 124.8, 126.1, 126.7, 128.6, 130.1, 135.4, 145.8, 152.1, 155.0, 191.7. MS (EI): *m/z* (%) 292 (10), 279 (5), 161 (100), 145 (7), 116 (7), 91 (8), 77 (1).

Monohydrazone of 4,4′-Bis(trifluoromethyl)benzil (4e). From **3e** (383 mg, 1.11 mmol) and $NH_2NH_2{\cdot}H_2O$ (111 mg, 2.22 mmol) in absolute EtOH (25 mL) was obtained **4e** (336 mg, 84%) as a white solid purified by flash chromatography (hexane/AcOEt 95:5).

General Procedure for the Preparation of Pyridazinones. Method A. EtOH, dried by distillation from Mg/I_2, was added to a flask containing Na (1.1 equiv) under argon atmosphere. After the Na reacted, a solution of ethyl cyanoacetate (1.1 equiv) in EtOH, dried by distillation from Mg/I_2, was added dropwise to the cold (0−5 °C) alkoxide solution. The solution was stirred at room temperature for 30 min. The corresponding monohydrazone (1 equiv) was then added as a solid. After the reaction mixture was heated at reflux temperature until the reaction was completed (TLC), it was cooled and poured into 1 N HCl. The formed precipitated was separated by filtration and purified by recrystallization from the appropriate solvent or by column chromatography using the appropriate eluents.

5,6-Bis(*p*-*tert*-butylphenyl)-4-cyanopyridazin-3(2*H*)-one (5d). From Na (108 mg, 4.70 mmol) in EtOH (25 mL), ethyl cyanoacetate (530 mg, 4.70 mmol) in EtOH (10 mL), and **4d** (1.43 g, 4.26 mmol) was obtained **5d** (1.60 g, 96%) as a white solid, mp >300 °C (AcOEt/cyclohexane). IR (KBr): 1655, 2220 cm^{-1}. ^1H NMR ($CDCl_3$): δ 1.27 (9H, s, $3CH_3$), 1.31 (9H, s, $3CH_3$), 7.01 (2H, d, J = 8.2, ArH), 7.15 (2H, d, J = 8.2, ArH), 7.23 (2H, d, J = 8.2, ArH), 7.37 (2H, d, J = 8.8, ArH), 11.63 (1H, sa, NH). ^{13}C NMR ($CDCl_3$): δ 31.0, 31.1, 34.6, 34.9, 113.1, 113.8, 125.1, 125.6, 128.8, 129.5, 131.1, 147.5, 152.5, 152.7, 154.2, 158.3. MS (EI): *m/z* (%) 385 (M^+, 36), 370 (100), 355 (1), 340 (1), 328 (3), 314 (11), 272 (4), 91 (2), 57 (24).

4-Cyano-5,6-bis(*p*-trifluoromethylphenyl)pyridazin-3(2*H*)-one (5e). From Na (233 mg, 1.01 mmol) in EtOH (15 mL), ethyl cyanoacetate (114 mg, 1.01 mmol) in EtOH (10 mL), and **4e** (330 mg, 0.92 mmol) was obtained **5e** (339 mg, 90%) as a white solid, mp 231−233 °C (toluene/hexane).

4-Cyano-5,6-bis(*p*-methoxyphenyl)pyridazin-3(2*H*)-one (5f).[24] From Na (180 mg, 7.70 mmol) in EtOH (75 mL), ethyl cyanoacetate (0.87 g, 7.70 mmol) in EtOH (10 mL), and monohydrazone of 4,4′-dimethoxybenzil[23] (2.0 g, 7.00 mmol) was obtained **5f** (2.0 g, 86%) as a yellow solid, mp 235−273 °C (absolute EtOH).

Method B. Cyanoacetohydrazide (2 equiv) was added in portions to a solution of the corresponding diketone (1 equiv) in absolute EtOH. The mixture was heated at reflux temperature until the reaction was completed (TLC). After the solution was cooled, the formed solid was isolated by filtration and purified by recrystallization from the appropriate solvent or by column chromatography using the appropriate eluents.

4-Cyano-5,6-di(2-furyl)pyridazin-3(2*H*)-one (5h). From 2,2′-furyl (1.5 g, 7.90 mmol) in absolute EtOH (30 mL) and cyanoacetohydrazide (1.56 g, 15.8 mmol) was obtained **5h** (1.1 g, 54%) as a brown solid purified by flash chromatography (hexane/AcOEt 9:1), mp 250−253 °C (absolute EtOH).

4-Cyano-5,6-di(2-pyridyl)pyridazin-3(2*H*)-one (5i). From 1,2-di(2-pyridyl)ethane-1,2-dione (2 g, 9.5 mmol) in absolute EtOH (75 mL) and cyanoacetohydrazide (1.68 g, 0.017 mmol) was obtained **5i** (538 mg, 21%) as a white solid purified by flash chromatography ($CHCl_3$/MeOH 98:2), mp 198 °C (dec). The mother liquor was concentrated and the crude product was purified by flash chromatography ($CHCl_3$/MeOH 95:5) to give 3-amino-4,5-di(2-pyridyl)-1*H*-pyrazolo[3,4-*c*]pyridazine **1i** (429 mg, 16%) as a yellow solid, mp 264 °C (dec) (absolute EtOH). IR (KBr): 3110, 3200, 3280, 3380, 3440 cm^{-1}. ^1H NMR (DMSO-d_6): δ 6.18 (2H, sa, NH_2), 6.72 (1H, dd, J = 6.7, 9.1, pyridylH), 6.92 (1H, m, pyridylH), 7.54 (1H, m, pyridylH), 7.87 (2H, m, pyridylH), 7.99 (1H, m, pyridylH), 8.14 (1H, d, J = 6.7, pyridylH), 8.78 (1H, d, J = 4.9, pyridylH), 11.90 (1H, sa, NH). ^{13}C NMR (DMSO-d_6): δ 98.6, 103.4, 113.8, 116.0, 119.9, 120.8, 122.1, 123.2, 124.0, 131.3, 137.3, 143.0, 148.4, 155.5, 160.3. MS (EI): *m/z* (%) 277 (100). Anal. ($C_{15}H_{17}N_7$) C, H, N.

Method C. To a solution of the corresponding diketone (1 equiv) in DMF was added, at 80 °C, a solution of cyanoacetohydrazide (2 equiv) in DMF. The mixture was heated at 100 °C until the reaction was completed (TLC). Then the solution was concentrated under vacuum. The residue was purified by recrystallization from the appropriate solvent or by column chromatography using the appropriate eluents.

5,6-Bis(4-biphenyl)-4-cyanopyridazin-3(2*H*)-one (5g). From 4,4′-diphenylbenzil[10] (1.34 g, 3.70 mmol) in DMF (15 mL) and cyanoacetohydrazide (0.73 mg, 7.37 mmol) in DMF (6 mL) was obtained **5g** (786 mg, 50%) as a yellow solid, mp >300 °C (dioxane).

4-Cyano-5,6-bis(*p*-nitrophenyl)pyridazin-3(2*H*)-one (5c). From 4,4′-dinitrobenzil[11] (2 g, 6.67 mmol) in DMF (15 mL) and cyanoacetohydrazide (1.32 g, 13.33 mmol) in DMF (10 mL) was obtained **5c** (1.3 g, 54%) as a yellow solid purified by flash chromatography (CH_2Cl_2/MeOH 99:1), mp >300 °C.

4-Cyano-5-phenylpyridazin-3(2*H*)-one (5l).[25] EtOH (44 mL), dried by distillation from Mg/I_2, was added to a flask

containing Na (270 mg, 11.74 mmol) under argon atmosphere. After the Na reacted, a solution of **7** (1.26 g, 5.86 mmol) in EtOH (25 mL) was added dropwise to the cold (0−5 °C) alkoxide solution. The solution was heated at reflux temperature for 3 h. After the solution was cooled, the solvent was removed under reduced pressure, the residue was dissolved in water (10 mL), and the pH was adjusted to 5 with 6 N HCl. The precipitate was isolated by filtration and purified by recrystallization from AcOEt/hexane to give **5l** (782 mg, 68%) as a brown solid, mp 218−220 °C.

Ethyl 6-(2-Furyl)-3-oxo-2,3,4,5-tetrahydropyridazine-4-carboxylate (9o). To a solution of 8.11 g (30.23 mmol) of **8o** in 60 mL of absolute EtOH cooled to 0 °C was added dropwise 15.13 g (30.23 mmol) of $NH_2NH_2 \cdot H_2O$ with stirring. The solution was heated at reflux temperature for 3 h. After the solution was cooled, the solvent was removed under reduced pressure. The crude of the reaction was purified by flash chromatography on silica gel (hexane/AcOEt 1:1) to give **9o** (3.3 g, 46%) as a white solid, mp 131−132 °C. IR (KBr): 1670, 1730, 3100, 3220 cm^{-1}. ^1H NMR ($CDCl_3$): δ 1.29 (3H, t, J = 7.1, CH_3), 3.06 (1H, dd, J = 17.0 and 6.6, CH_AH_B), 3.34 (1H, dd, J = 17.0 and 8.8, CH_AH_B), 3.60 (1H, dd, J = 8.8 and 6.6, CH), 4.26 (2H, q, J = 7.1, OCH_2CH_3), 6.51 (1H, dd, J = 1.6 and 3.3, furylH), 6.80 (1H, d, J = 3.30, furylH), 7.54 (1H, d, J = 1.65, furylH), 8.86 (1H, s, NH). ^{13}C NMR ($CDCl_3$): δ 14.0, 25.2, 43.1, 62.3, 112.0, 142.6, 144.7, 149.2, 162.8, 167.7. MS (ESI): m/z 259 $[M + Na]^+$. Anal. ($C_{11}H_{12}N_2O_2$) C, H, N.

Ethyl 6-(2-Furyl)-3-oxo-2,3-dihydropyridazine-4-carboxylate (10o). To a solution of 3.07 g (13.00 mmol) of **9o** in 50 mL of acetic acid was added dropwise 0.65 mL (13.00 mmol) of bromine in 50 mL of acetic acid. The solution was stirred at room temperature for 2 h. Then, the solvent was removed under reduced pressure and the residue was dissolved in water. The crude of reaction was extracted with $CHCl_3$, and the collected organic layers were dried over $MgSO_4$ and concentrated to give a solid, which was purified by recrystallization from absolute ethanol to give **10o** (2.5 g, 83%) as a yellow solid, mp 177−179 °C. IR (KBr): 1600, 1660, 1710, 2020, 3120, 3140 cm^{-1}. ^1H NMR ($CDCl_3$): δ 1.43 (3H, t, J = 7.1, CH_3), 4.46 (2H, q, J = 7.1, CH_2), 6.55 (1H, dd, J = 3.3 and 1.7, furylH), 6.39 (1H, d, J = 3.3, furylH), 7.56 (1H, d, J = 1.6, furylH), 8.25 (1H, s, pyridazineH), 11.97 (1H, br s, NH). ^{13}C NMR ($CDCl_3$): δ 14.2, 62.4, 109.3, 112.4, 130.7, 132.2, 138.5, 144.1, 148.3, 158.1, 162.8. MS (ESI): m/z 257 $[M + Na]^+$. Anal. ($C_{11}H_{10}N_2O_4 \cdot 0.25H_2O$) C, H, N.

6-(2-Furyl)-3-oxo-2,3-dihydropyridazine-4-carboxamide (11o). A solution of 1.60 g (6.83 mmol) of **10o** in 60 mL of concentrated ammonia was stirred at room temperature for 18 h. Then, the solvent was removed under reduced pressure to give **110** (1.4 g, 99%) as a yellow solid, mp 313 °C (dec). IR (KBr): 1600, 1705, 3140, 3320 cm^{-1}. ^1H NMR (DMSO-d_6): δ 6.68 (1H, dd, J = 1.8 and 3.0, furylH), 7.19 (1H, d, J = 3.0, furylH), 7.88 (1H, d, J = 1.8, furylH), 8.12 (1H, s, NH_2), 8.40 (1H, s, pyridazineH), 8.84 (1H, s, NH_2). ^{13}C NMR (DMSO-d_6): δ 109.7, 112.4, 130.3, 130.7, 138.2, 144.8, 144.8, 148.4, 160.3, 162.4. MS (ESI): m/z 228 $[M + Na]^+$.

General Procedure for the Preparation of Cloropyridazines. A mixture of the corresponding pyridazinone, an excess of $POCl_3$, and dioxane was heated under reflux until the reaction was completed (TLC). The solution was cooled and poured into ice/water. The precipitated was isolated by filtration and purified by recrystallization from the appropriate solvent or by column chromatography using the appropriate eluents.

5,6-Bis(4-biphenyl)-3-chloropyridazine-4-carbonitrile (6b). From **5b** (560 mg, 1.32 mmol) and $POCl_3$ (4 mL, 43.56 mmol) in dioxane (17 mL) was obtained **6b** (288 mg, 50%) as a yellow solid, mp 226−229 °C (dioxane/absolute EtOH). IR (KBr): 2220 cm^{-1}. ^1H NMR (DMSO-d_6): δ 7.42 (8H, m, ArH), 7.55 (2H, d, J = 8.5, ArH), 7.68 (4H, m, ArH), 7.75 (2H, d, J = 7.0, ArH), 7.84 (2H, d, J = 7.9, ArH). ^{13}C NMR (DMSO-d_6): δ 113.2, 115.1, 126.3, 126.6, 126.7, 127.9, 128.1, 128.86, 128.92, 130.0, 130.3, 131.5, 133.7, 138.5, 138.7, 140.9, 141.5, 143.7, 153.0, 159.2. MS (EI): m/z (%) 445 (M^+ + 2, 44), 443 (M^+, 100), 408 (34), 382 (2), 366 (41).

5,6-Bis(*p*-*tert*-butylphenyl)-3-chloropyridazine-4-carbonitrile (6d). From **5d** (1.40 g, 3.64 mmol) and $POCl_3$ (11 mL, 120.12 mmol) in dioxane (35 mL) was obtained **6d** (1.15 g, 82%) as a yellow solid purified by flash chromatography (hexane/AcOEt 9:1), mp 182−184 °C.

3-Chloro-5,6-bis(*p*-nitrophenyl)pyridazine-4-carbonitrile (6c). From **5c** (461 mg, 1.27 mmol) and $POCl_3$ (9 mL, 101.60 mmol) in dioxane (10 mL) was obtained **6c** (254 mg, 52%) as a yellow solid purified by flash chromatography (hexane/AcOEt 8:2), mp 215−217 °C.

3-Chloro-5,6-bis(*p*-trifluoromethylphenyl)pyridazine-4-carbonitrile (6e). From **5e** (130 mg, 0.32 mmol) and $POCl_3$ (1 mL, 11.84 mmol) in dioxane (4 mL) was obtained **6e** (93 mg, 68%) as a white solid purified by flash chromatography (hexane/AcOEt 8:2).

3-Chloro-5,6-bis(*p*-methoxyphenyl)pyridazine-4-carbonitrile (6f). From **5f** (750 mg, 2.25 mmol) and $POCl_3$ (7 mL, 81.84 mmol) in dioxane (15 mL) was obtained **6f** (759 mg, 96%) as a yellow solid, mp 144−146 °C (absolute EtOH).

3-Chlorodibenzo[*f,h*]cinnoline-4-carbonitrile (6g). From 4-cyanodibenzo[*f,h*]cinnolin-3(2*H*)-one[26] (325 mg, 1.20 mmol) and $POCl_3$ (4 mL, 39.60 mmol) in dioxane (20 mL) was obtained **6g** (294 mg, 85%) as a yellow solid, mp 239−241 °C (dioxane).

3-Chloro-5,6-di(2-furyl)pyridazine-4-carbonitrile (6h). To a solution of **5h** (841 mg, 3.30 mmol) in dioxane (27 mL) was added dropwise, under argon atmosphere and at 0 °C, 10 mL (109.7 mmol) of $POCl_3$. The mixture was heated to reflux for 7 h. Then, the solution was cooled and poured into ice/water. The precipitate was isolated by filtration and purified by flash chromatography (hexane/AcOEt 9:1) to give **6h** (680 mg, 76%) as a yellow solid, mp 90−92 °C.

3-Chloro-6-methyl-5-phenylpyridazine-4-carbonitrile (6k). From 4-cyano-6-methyl-5-phenylpyridazin-3(2*H*)-one[26] (300 mg, 1.42 mmol) and $POCl_3$ (4 mL, 46.86 mmol) in dioxane (7 mL) was obtained **6k** (244 mg, 75%) as a brown solid, mp 125−127 °C (MeOH/H_2O).

3-Chloro-5-phenylpyridazine-4-carbonitrile (6l).[25] To a solution of **5l** (1.68 g, 8.52 mmol) in dioxane (25 mL) was added 26 mL (281 mmol) of $POCl_3$. The mixture was heated to reflux for 3 h, and then the solution was cooled and poured into ice/water. The precipitate was collected by filtration, and the combined filtrates were concentrated under reduced pressure and purified by flash chromatography on silica gel (hexane/AcOEt 99:1) to give **6l** (108 mg, 6%) as a brown solid, mp 105−108 °C.

3-Chloro-6-(2-furyl)pyridazine-4-carbonitrile (6o). From **11o** (1.58 g, 7.70 mmol) and $POCl_3$ (17 mL, 183.73 mmol) in dioxane (30 mL) was obtained **6o** (1.26 g, 80%) as a yellow solid purified by flash chromatography (hexane/AcOEt 7:3), mp 168−169 °C.

General Procedure for the Preparation of Pyrazolo[3,4-*c*]pyridazines. To a solution of the corresponding cloropyridazine in absolute EtOH was added an excess of hydrazine hydrate in absolute EtOH. The mixture was heated at reflux temperature until the reaction was completed (TLC). After the solution was cooled, the formed solid was isolated by filtration and purified by recrystallization from the appropriate solvent or by column chromatography using the appropriate eluents.

3-Amino-4,5-bis(4-biphenyl)-1*H*-pyrazolo[3,4-*c*]pyridazine (1b). From **6b** (250 mg, 0.56 mmol) and $NH_2NH_2 \cdot H_2O$ (42 mg, 0.84 mmol) in absolute EtOH (5 mL) was obtained **1b** (194 mg, 79%) as a yellow solid, mp >300 °C (DMF/AcOEt). IR (KBr): 3160, 3300, 3430 cm^{-1}. ^1H NMR (DMSO-d_6): δ 4.75 (2H, sa, NH_2), 7.42 (10H, m, ArH), 7.64 (4H, m, ArH), 7.78 (4H, m, ArH), 13.10 (1H, sa, NH). ^{13}C NMR (DMSO-d_6): δ 105.9, 126.0, 126.6, 126.7, 127.6, 128.0, 129.0, 129.1, 130.1, 130.2, 130.9, 131.9, 132.5, 136.8, 138.90, 138.91, 139.3, 140.1, 147.7, 149.6, 154.5. MS (EI): m/z (%) 439 (M^+, 100), 362 (32). Anal. ($C_{29}H_{21}N_5$) C, H, N.

3-Amino-4,5-bis(*p*-*tert*-butylphenyl)-1*H*-pyrazolo[3,4-*c*]-pyridazine (1d). From **6d** (1.15 g, 2.85 mmol) and $NH_2NH_2 \cdot$

H_2O (360 mg, 7.20 mmol) in absolute EtOH (45 mL) was obtained **1d** (800 mg, 70%) as a yellow solid, mp >300 °C (absolute EtOH).

3-Amino-4,5-bis(*p*-nitrophenyl)-1*H*-pyrazolo[3,4-*c*]pyridazine (1c). From **6c** (271 mg, 0.71 mmol) and $NH_2NH_2{\cdot}H_2O$ (53 mg, 1.07 mmol) in absolute EtOH (6 mL) was obtained **1c** (166 mg, 62%) as a yellow solid purified by flash chromatography (CH_2Cl_2/hexane 8:2), mp >300 °C (AcOEt).

3-Amino-4,5-bis(*p*-trifluoromethylphenyl)-1*H*-pyrazolo[3,4-*c*]pyridazine (1e). From **6e** (180 mg, 0.42 mmol) and $NH_2NH_2{\cdot}H_2O$ (42 mg, 0.84 mmol) in absolute EtOH (10 mL) was obtained **1e** (120 mg, 67%) as a yellow solid purified by flash chromatography ($CHCl_3$/MeOH 99:1), mp 162−163 °C (absolute EtOH).

3-Amino-4,5-bis(*p*-methoxyphenyl)-1*H*-pyrazolo[3,4-*c*]-pyridazine (1f). From **6f** (300 mg, 0.85 mmol) and $NH_2NH_2{\cdot}H_2O$ (214 mg, 4.27 mmol) in absolute EtOH (25 mL) was obtained **1f** (286 mg, 97%) as a yellow solid purified by flash chromatography ($CHCl_3$/AcOEt 8:2), mp 129−130 °C (absolute EtOH).

3-Amino-4,5-di(2-furyl)-1*H*-pyrazolo[3,4-*c*]pyridazine (1h). From **6h** (200 mg, 0.74 mmol) and $NH_2NH_2{\cdot}H_2O$ (55 mg, 1.11 mmol) in absolute EtOH (6 mL) was obtained **1h** (136 mg, 69%) as a brown solid purified by flash chromatography ($CHCl_3$/MeOH 95:5), mp 250−252 °C (absolute EtOH).

3-Amino-5-methyl-4-phenyl-1*H*-pyrazolo[3,4-*c*]pyridazine (1k). From **6k** (300 mg, 1.31 mmol) and $NH_2NH_2{\cdot}H_2O$ (98 mg, 1.96 mmol) in absolute EtOH (11 mL) was obtained **1k** (161 mg, 55%) as a yellow solid purified by flash chromatography (AcOEt/hexane 9:1), mp 122−127 °C (AcOEt).

3-Amino-4-phenyl-1*H*-pyrazolo[3,4-*c*]pyiridazine (1l).[25] From **6l** (35 mg, 0.16 mmol) and $NH_2NH_2{\cdot}H_2O$ (12 mg, 0.24 mmol) in absolute EtOH (2 mL) was obtained **1l** (30 mg, 88%) as a yellow solid purified by flash chromatography (HCl_3/MeOH 99:1), mp 219−221 °C (AcOEt).

3-Amino-5-phenyl-1*H*-pyrazolo[3,4-*c*]pyiridazine (1n).[27] From 3-chloro-6-phenylpyridazine-4-carbonitrile **20**[28] (300 mg, 1.40 mmol) and $NH_2NH_2{\cdot}H_2O$ (105 mg, 2.10 mmol) in absolute EtOH (12 mL) was obtained **1n** (193 mg, 96%) as a yellow solid purified by flash chromatography ($CHCl_3$/EtOH 9:1), mp >300 °C (H_2O).

3-Amino-5-(2-furyl)-1*H*-pyrazolo[3,4-*c*]pyiridazine (1o). From **6o** (206 mg, 1.00 mmol) and $NH_2NH_2{\cdot}H_2O$ (101 mg, 2.00 mmol) in absolute EtOH (12 mL) was obtained **1o** (193 mg, 96%) as a yellow solid purified by flash chromatography ($CHCl_3$/EtOH 9:1), mp 206−208 °C (H_2O).

3-Amino-4,5-bis(*p*-aminophenyl)-1*H*-pyrazolo[3,4-*c*]-pyridazine (1m). A solution of **1c** (85 mg, 0.23 mmol) in a mixture of THF (3.5 mL) and MeOH (1.5 mL) was added dropwise to a solution of $NH_2NH_2{\cdot}H_2O$ (310 mg, 6.20 mmol) and Raney nickel (57 mg) in absolute MeOH (2 mL) under argon atmosphere. The mixture was heated at reflux temperature for 1 h, and Raney nickel was separated by filtration and washed with MeOH. The combined filtrates were concentrated under reduced pressure, and the residual solid was crystallized from MeOH to give **1m** (38 mg, 52%), mp 227 °C (dec).

1-Amino-3*H*-dibenzo[*f,h*]pyrazolo[3,4-*c*]cinnoline (1g). To a solution of **6g** (313 mg, 1.08 mmol) in DMF (15 mL) was added 81 mg (1.62 mmol) of $NH_2NH_2{\cdot}H_2O$. The mixture was heated at 110 °C for 8 h. Then, the solution was cooled and poured into ice/water. The precipitate was isolated by filtration and purified by recrystallization from DMF/H_2O to give **1g** (150 mg, 50%), mp 235−239 °C.

General Procedure for the Preparation of Ureas. To a solution of the corresponding isocyanate in anhydrous CH_2Cl_2 was added, at 0 °C, a solution of the corresponding aminopyrazolo[3,4-*c*]pyridazine in a mixture of CH_2Cl_2/THF 5:3. The mixture was stirred at room temperature for 20 h. Then, the desired compound was isolated by filtration or concentrated the solvent under vacuum.

1-(4,5-Diphenyl-1*H*-pyrazolo[3,4-*c*]pyridazin-3-yl)-3-ethylurea (2b). From ethyl isocyanate (48 mg, 0.68 mmol) in anhydrous CH_2Cl_2 (1 mL) and **1a**[20] (180 mg, 0.68 mmol) in a mixture of CH_2Cl_2/THF 5:3 (8 mL) was obtained **2b** (174 mg, 72%) as a red solid isolated by concentrating the solvent under vacuum, mp 132−134 °C. IR (KBr): 1715, 3310, 3350, 3460 cm^{-1}. ^1H NMR ($CDCl_3$): δ 1.30 (3H, t, J = 7.1, CH_3), 3.51 (2H, m, CH_2), 6.23 (2H, sa, 2NHCO), 7.23−7.47 (10H, m, ArH), 7.94 (1H, sa, NH). ^{13}C NMR ($CDCl_3$): δ 14.5, 35.3, 127.4, 127.8, 128.8, 129.2, 129.3, 130.2, 133.3, 136.7, 144.8, 147.3, 152.8. MS (EI): *m/z* (%) 316 (M^+ − 42, 26), 288 (100), 72 (32).

1-(4,5-Diphenyl-1*H*-pyrazolo[3,4-*c*]pyridazin-3-yl)-3-phenylurea (2c). From phenyl isocyanate (0.076 mL, 0.70 mmol) in anhydrous CH_2Cl_2 (1 mL) and **1a**[20] (200 mg, 0.70 mmol) in a mixture of CH_2Cl_2/THF 5:3 (5 mL) was obtained **2c** (94 mg, 33%) as a yellow solid isolated by filtration, mp 239−241 °C.

1-Ethyl-3-[5-(2-furyl)1-*H*-pyrazolo[3,4-*c*]pyridazin-3-yl]-urea (13). To a solution of ethyl isocyanate (71 mg, 1.00 mmol) in anhydrous THF (5 mL) was added at 0 °C a solution of **1o** (201 mg, 1.00 mmol) in anhydrous THF (10 mL). The mixture was stirred at room temperature for 24 h. Then, the solvent was removed under reduced pressure and the crude of reaction was purified by flash chromatography on silica gel ($CHCl_3$/EtOH 9.9:0.1) to give **13** (150 mg, 55%) as a red solid, mp 172−174 °C.

1-Ethyl-3-[5-(2-furyl)-1*H*-pyrazolo[3,4-*c*]pyridazin-3-yl]-thiourea (14). The starting materials were ethyl isothiocyanate (87 mg, 1.00 mmol) in anhydrous CH_2Cl_2 (5 mL) and **1o** (201 mg, 1.00 mmol) in a mixture of CH_2Cl_2/THF 5:3 (10 mL). After 20 h, the solvent was removed under reduced pressure and the crude of reaction was purified by flash chromatography on silica gel ($CHCl_3$/EtOH 9:1) to give **14** (80 mg, 28%) as a yellow solid, mp 240−242 °C.

(4,5-Diphenyl-1*H*-pyrazolo[3,4-*c*]pyridazin-3-yl)hydrazine Trihydrochloride (2d). A suspension of **1a**[20] (0.50 g, 1.74 mmol) in H_2O (2 mL) was added dropwise to a solution of $NaNO_2$ (120 mg, 1.74 mmol) and concentrated HCl in H_2O (2 mL) at 0 °C for 48 h. After cooling, the formed solid was filtered under vacuum and purified by recrystallization from absolute EtOH to give **2d** (760 mg, 75%), mp 134−136 °C. IR (KBr): 3190, 3290, 3440 cm^{-1}. ^1H NMR ($CDCl_3$): δ 3.46 (1H, sa, OH), 3.70 (4H, sa, $2CH_2$), 3.91 (2H, sa, NH_2), 4.04 (2H, t, J = 5.0, CH_2), 4.76 (2H, t, J = 5.0, CH_2), 7.24−7.42 (10H, m, ArH). ^{13}C NMR ($CDCl_3$): δ 46.7, 61.6, 69.5, 72.6, 107.1, 127.6, 127.8, 128.7, 129.1, 129.4, 130.4, 132.5, 133.4, 136.9, 146.3, 151.0, 152.8. MS (ESI): *m/z* 398 $[M + Na]^+$. Anal. ($C_{21}H_{21}N_5O_2$) C, H, N.

3-Acetamide-4,5-diphenyl-1*H*-pyrazolo[3,4-*c*]pyridazine (2e). A mixture of **1a**[20] (200 mg, 0.70 mmol), acetyl chloride (157 mg, 2.00 mmol), and two drops of Et_3N in dioxane (4 mL) was heated under reflux for 30 min. Then, the solvent was removed under reduced pressure and the crude of reaction was purified by flash chromatography on silica gel ($CHCl_3$/MeOH 99:1) to give **2e** (180 mg, 78%) as a white solid, mp 262−264 °C (lit.[29] mp 228−229 °C, absolute EtOH/toluene). IR (KBr): 1670, 3185, 3210, 3440 cm^{-1}. ^1H NMR (DMSO-d_6): δ 1.48 (3H, s, CH_3), 7.15 (2H, m, ArH), 7.30 (8H, m, ArH), 9.81 (1H, s, NHCO), 12.92 (1H, s, NH). ^{13}C NMR (DMSO-d_6): δ 21.9, 110.6, 127.69, 127.74, 127.9, 128.3, 129.9, 130.5, 131.8, 132.7, 137.5, 138.6, 152.0, 154.9, 170.0. MS (EI): *m/z* (%) 329 (M^+, 43), 286 (100), 77 (9), 51 (6). Anal. ($C_{19}H_{15}N_5O$) C, H, N.

1-Acetyl-3-amino-4,5-diphenyl-1*H*-pyrazolo[3,4-*c*]pyridazine (2f). A mixture of **1a**[20] (400 mg, 1.39 mmol) and acetyl chloride (0.14 mL, 1.96 mmol) in pyridine (3 mL) was heated under reflux for 1 h. Then, the pH was adjusted to 5 with aqueous hydrochloric acid. The precipitate formed was collected by filtration to give **2f** (305 mg, 66%) as a brown solid, mp 246−248 °C (toluene). IR (KBr): 1695, 3195, 3250, 3485 cm^{-1}. ^1H NMR (DMSO-d_6): δ 2.77 (3H, s, CH_3), 5.31 (2H, s, NH_2), 7.35 (7H, m, ArH), 7.48 (3H, m, ArH). ^{13}C NMR (DMSO-d_6): δ 24.4, 112.5, 127.9, 128.2, 128.8, 129.3, 129.4, 130.1, 131.8, 133.1, 136.5, 149.6, 153.3, 154.6, 167.0. Anal. ($C_{19}H_{15}N_5O$) C, H, N.

3-Acetamide-1-acetyl-4,5-diphenyl-1*H*-pyrazolo[3,4-*c*]-pyridazine (2g). A mixture of **1a**[20] (200 mg, 0.70 mmol) in acetic anhydride (1 mL) and acetic acid (1 mL) was heated

under reflux for 90 min. Then, the solution was cooled and poured into ice/water. The precipitate was isolated by filtration and purified by recrystallization to give **2g** (150 mg, 58%) as a white solid, mp 174−175 °C (AcOEt/hexane). IR (KBr): 1785, 3160, 3550 cm^{-1}. ^1H NMR (DMSO-d_6): δ 1.46 (3H, s, CH_3-CONH), 2.90 (3H, s, CH_3CON), 7.17 (2H, m, ArH), 7.35 (8H, m, ArH), 10.32 (1H, sa, NH). ^{13}C NMR (DMSO-d_6): δ 21.7, 24.3, 114.9, 127.7, 127.9, 128.2, 128.6, 129.9, 130.2, 131.6, 133.1, 136.6, 142.8, 153.7, 155.4, 167.3, 169.8.

3-Amino-1-benzyl-4,5-diphenyl-1*H*-pyrazolo[3,4-*c*]pyridazine (2h). To a solution of **6a**[20] (500 mg, 1.72 mmol) in absolute EtOH (20 mL) was added 667 mg (3.42 mmol) of benzylhydrazine and 0.71 mL (5.13 mmol) of Et_3N. The mixture was stirred at reflux temperature for 24 h. Then, the solvent was removed under reduced pressure and the crude of reaction was purified by flash chromatography on silica gel ($CHCl_3$/EtOH 20:1) to give **2h** (225 mg, 35%) as a yellow solid, mp 167−169 °C (AcOEt/hexane). IR (KBr): 3180, 3280, 3450 cm^{-1}. ^1H NMR (DMSO-d_6): δ 3.87 (2H, sa, NH_2), 5.73 (2H, s, CH_2), 7.26−7.52 (15H, m, ArH). ^{13}C NMR (DMSO-d_6): δ 50.7, 106.9, 127.6, 127.8, 128.4, 128.6, 128.7, 129.0, 129.4, 130.4, 130.8, 132.3, 133.5, 136.8, 137.0, 146.4, 151.0, 152.6. Anal. ($C_{24}H_{19}N_5$) C, H, N.

2-[(3-Amino-4,5-diphenyl-1*H*-pyrazolo[3,4-*c*]pyridazin-1-yl)methoxy]ethyl Acetate (12i). Cs_2CO_3 (284 mg, 0.87 mmol) was added in portions to a solution of **1a** [20] (250 mg, 0.87 mmol) in DMF (6 mL). The mixture was stirred at room temperature for 30 min. Then, 2-bromomethoxyethyl acetate[14] (172 mg, 0.87 mmol) was added and the solution was stirred for 24 h. Then, the solvent was eliminated under vacuum and the formed solid was extracted with AcOEt. The combined extracts were dried over $MgSO_4$ and concentrated to give a solid, which was purified by flash chromatography (CH_2Cl_2/MeOH 98:2) to give **12i** (122 mg, 35%), mp 143−144 °C (AcOEt/hexane). IR (KBr): 1740, 3340, 3470 cm^{-1}. ^1H NMR ($CDCl_3$): δ 2.07 (3H, s, CH_3), 3.90 (2H, dd, J = 4.4, 4.9, CH_2), 3.97 (2H, sa, NH_2), 4.23 (2H, dd, J = 4.4, 4.9, CH_2), 5.97 (2H, s, CH_2N), 7.25−7.44 (10H, m, ArH). ^{13}C NMR ($CDCl_3$): δ 20.8, 63.1, 67.4, 75.5, 107.9, 127.7, 127.8, 128.7, 129.1, 129.3, 130.2, 132.5, 133.0, 136.6, 147.2, 152.0, 153.4, 170.8. Anal. ($C_{22}H_{21}N_5O_3$) C, H, N. Further elution afforded 127 mg (51%) of **1a**.[20]

2-[2-(3-Amino-4,5-diphenyl-1*H*-pyrazolo[3,4-*c*]pyridazin-1-yl)ethoxy]ethyl Acetate (12j). Cs_2CO_3 (1.14 g, 3.49 mmol) was added in portions to a solution of **1a**[20] (1.00 g, 3.49 mmol) in DMF (24 mL). The mixture was stirred at room temperature for 30 min. Then, 2-(2-iodoethoxy)ethyl acetate[30] (900 mg, 3.49 mmol) was added and the solution was stirred for 24 h. Then, the solvent was eliminated under vacuum and the formed solid was extracted with AcOEt. The combined extracts were dried over $MgSO_4$ and concentrated to give a solid, which was purified by flash chromatography ($CHCl_3$/EtOH 9:1) to give **12j** (1.14 g, 78%), mp 157−159 °C (AcOEt). IR (KBr): 1730, 3340, 3485 cm^{-1}. ^1H NMR ($CDCl_3$): δ 2.02 (3H, s, CH_3), 3.75 (2H, t, J = 4.9, CH_2), 3.88 (2H, sa, NH_2), 4.05 (2H, t, J = 5.5, CH_2), 4.17 (2H, m, CH_2), 4.75 (2H, t, J = 5.5, CH_2), 7.25−7.42 (10H, m, ArH). ^{13}C NMR ($CDCl_3$): δ 20.8, 46.2, 63.4, 68.5, 68.9, 106.9, 127.5, 127.8, 128.7, 129.0, 129.4, 130.3, 132.2, 133.5, 137.0, 146.1, 150.9, 152.9, 170.9. Anal. ($C_{23}H_{23}N_5O_3$) C, H, N.

2-[(3-Amino-4,5-diphenyl-1*H*-pyrazolo[3,4-*c*]pyridazin-1-yl)methoxy]ethanol (2i). A solution of **12i** (2.24 g, 5.56 mmol) in 1 N NH_4OH (24 mL) was heated at 50−60 °C for 24 h. After the mixture was cooled, the formed solid was filtered under vacuum and purified by flash chromatography ($CHCl_3$/EtOH 9:1) to give **2i** (1.40 g, 70%), mp 178−181 °C (absolute EtOH). IR (KBr): 3295, 3330, 3430 cm^{-1}. ^1H NMR ($CDCl_3$): δ 3.76 (2H, m, CH_2), 3.84 (2H, m, CH_2), 4.00 (2H, sa, NH_2), 5.99 (2H, s, CH_2N), 7.27−7.44 (10H, m, ArH). ^{13}C NMR ($CDCl_3$): δ 61.9, 71.2, 75.9, 108.2, 127.9, 128.0, 128.9, 129.3, 129.5, 130.4, 132.8, 133.2, 136.7, 147.4, 152.2, 153.6. MS (ESI): m/z 384 $[M + Na]^+$. Anal. ($C_{20}H_{19}N_5O_2$) C, H, N.

2-[2-(3-Amino-4,5-diphenyl-1*H*-pyrazolo[3,4-*c*]pyridazin-1-yl)ethoxy]ethanol (2j). A solution of **12j** (1.12 g, 2.69 mmol) in 1 N NH_4OH (60 mL) was heated at 50−60 °C for 48 h. After the mixture was cooled, the formed solid was filtered under vacuum and purified by recrystallization from absolute EtOH to give **2j** (760 mg, 75%), mp 134−136 °C. IR (KBr): 3190, 3290, 3440 cm^{-1}. ^1H NMR ($CDCl_3$): δ 3.46 (1H, sa, OH), 3.70 (4H, sa, $2CH_2$), 3.91 (2H, sa, NH_2), 4.04 (2H, t, J = 5.0, CH_2), 4.76 (2H, t, J = 5.0, CH_2), 7.24−7.42 (10H, m, ArH). ^{13}C NMR ($CDCl_3$): δ 46.7, 61.6, 69.5, 72.6, 107.1, 127.6, 127.8, 128.7, 129.1, 129.4, 130.4, 132.5, 133.4, 136.9, 146.3, 151.0, 152.8. MS (ESI): m/z 398 $[M + Na]^+$. Anal. ($C_{21}H_{21}N_5O_2$) C, H, N.

CDK1/Cyclin B Enzyme Inhibition. Biochemical Reagents. Sodium orthovanadate, EGTA, EDTA, Mops, β-glycerophosphate, phenyl phosphate, sodium fluoride, dithiothreitol (DTT), glutathione agarose, glutathione, bovine serum albumin (BSA), nitrophenyl phosphate, leupeptin, aprotinin, pepstatin, soybean trypsin inhibitor, benzamidine, and histone H1 (type III-S) were obtained from Sigma Chemicals. [γ-^{32}P]-ATP (PB 168) was obtained from Amersham.

The GS-1 peptide (YRRAAVPPSPSLSRHSSPHQSpEDEEE) was synthesized by the Peptide Synthesis Unit, Institute of Biomolecular Sciences, University of Southampton, Southampton SO16 7PX, U.K.

Buffers. Homogenization buffer consisted of 60 mM β-glycerophosphate, 15 mM *p*-nitrophenyl phosphate, 25 mM Mops (pH 7.2), 15 mM EGTA, 15 mM $MgCl_2$, 1 mM DTT, 1 mM sodium vanadate, 1 mM NaF, 1 mM phenyl phosphate, 10 μg of leupeptin/mL, 10 μg of aprotinin/mL, 10 μg of soybean trypsin inhibitor/mL, and 100 μM benzamidine. Buffer A consisted of 10 mM $MgCl_2$, 1 mM EGTA, 1 mM DTT, 25 mM Tris-HCl, pH 7.5, 50 μg of heparin/mL. Buffer C was the same as the homogenization buffer but with 5 mM EGTA, no NaF, and no protease inhibitors.

Kinase Preparations and Assays. Kinase activities were assayed in buffer A or C (unless otherwise stated), at 30 °C, at a final ATP concentration of 15 μM. Blank values were subtracted and activities calculated as pmoles of phosphate incorporated for a 10 min incubation. The activities are usually expressed in percent of the maximal activity, i.e., in the absence of inhibitors. Controls were performed with appropriate dilutions of dimethyl sulfoxide.

CDK1/cyclin B was extracted in homogenization buffer from M. phase starfish (*Marthasterias glacialis*) oocytes and purified by affinity chromatography on $p9^{CKShs1}$-sepharose beads, from which it was eluted by free $p9^{CKShs1}$ as previously described.[15] The kinase activity was assayed in buffer C, with 1 mg of histone H1/mL, in the presence of 15 μM [γ-^{33}P]ATP (3000 Ci/mmol, 1 mCi/mL) in a final volume of 30 μL. After 10 min of incubation at 30 °C, 25 μL aliquots of supernatant were spotted onto P81 phosphocellulose papers and treated as described above.

In Vitro Cytotoxicity Assays. The cell lines used were human colon carcinoma (HT-29) (ATCC, HTB 38), human cervical carcinoma (HeLa) (ATCC, CCL 2), and human prostate carcinoma (PC-3) (ECACC, 90112714). For each experiment, cultures were seeded from frozen stocks. Each cell line was maintained in its appropriate medium and was incubated at 37 °C in a 5% CO_2 atmosphere.

All cell lines were in the logarithmic phase of growth when the assay of 3-(4,5-dimethylthiazol-2-yl)-2,5-diphenyltetrazolium bromide (MTT) was carried out. Cells were harvested and seeded into 96-well tissue culture plates at a density of 2.5×10^3 cells/well in 150 μL aliquots of medium. The concentrations tested were serial dilutions of a stock solution (1×10^{-5} M in DMSO) with phosphate-buffered saline (PBS) and were added 24 h later. The assay was ended after 72 h of drug exposure, and PBS was used as a negative control and doxorubicine as a positive control.

After a 72 h exposure period, cells were washed twice with PBS, and then 50 μL/well of MTT reagent (1 mg/mL in PBS; Sigma) and 150 μL/well of prewarmed medium were added. The plates were returned to the incubator for 4 h. Subsequently, DMSO was added as solvent. Absorbance was determined at 570 nm with a microplate reader (Opsys MR).

All experiments were performed at least three times, and the average of the percentage absorbance was plotted against

concentration. Then, the concentration of drug required to inhibit 50% of cell growth (IC_{50}) was calculated for each compound.

Computational Details. Molecular Modeling and Conformational Searches. Compounds **1a** and the synthetic derivatives (**1b**−**n** and **2a**−**c**,**e**,**f**) were model built in SYBYL 6.7[31] using standard geometries. Conformational searches and energy minimizations were performed using Macromodel, version 5.5.[32] The Macromodel implementation of the AMBER[33] all-atom force field was used (denoted AMBER*). All calculations were performed using the implicit water GB/SA solvation model of Still et al.[34] Conformational searches were performed using the Monte Carlo method of Goodman and Still.[35] For each search 1000 starting structures were generated and minimized to an energy convergence of 0.05 (kJ/mol)/Å using the Polak−Ribiere conjugate gradient minimization method implemented in Macromodel. Duplicated structures and those greater than 50 kJ/mol above the global minimum were discarded. The lowest energy conformer for each compound was then fully optimized by means of the ab initio quantum mechanical program Gaussian 98[36] and the 3-21G basis set. RHF/6-31G*//3-21G RESP charges[37] were derived together with appropriate bonded and nonbonded parameters consistent with the AMBER force field[38] (Tables 3 and 4 in Supporting Information). These low-energy minimized conformers were selected to be used as input for the ligand docking process.

CDK2 Model Building and Energy Refinement. For the flexible ligand docking the CDK2-ATP complex structure was directly retrieved from the Protein Data Bank (PDB)[39] (code 1hck). The ATP molecule, the magnesium ion, and water molecules were manually removed. Polar hydrogens and Kollman united-atom partial atomic charges were added by means of the SYBYL program.[31] For the molecular dynamics simulations the same starting structure was used; however, some preliminary model building and energy refinement had to be undertaken. The 10 missing amino acids from the 1hck crystal structure (Ala31 through Thr41) were directly taken from the CDK2/cyclin A/ATP complex (code 1fin) after superimposition of common parts in both structures. Hydrogens were added using standard geometries, and their positions were optimized using the molecular mechanics program AMBER.[40] A short optimization was then undertaken where only the residues connecting the added residues were allowed to move (Thr39 through Val44 and Glu28 through Lys33) in a continuum medium of relative permittivitty $\epsilon = 4r_{ij}$ for imitating the solvent environment. Finally, an optimization run restraining all non-H atoms to their initial coordinates allowed readjustment of covalent bonds and van der Waals contact without changing the overall conformation of the protein, which was considered the starting structure for the molecular dynamics simulations described below.

Docking. All docking studies were performed with the program AutoDock (version 3.0).[41] The target in each docking run was CDK2 obtained as described above. Affinity grid files were generated using the auxiliary program AUTOGRID (version 3.0). The center of the removed ATP molecule bound to the active site was chosen as the center of the grids, and the dimensions of the grid were $60 \times 60 \times 60$ Å^3 with grid points separated by 0.375 Å. The original Lennard-Jonnes and hydrogen-bonding potentials provided by the program were used. The parameters for the docking using the Lamarckian genetic algorithm (LGA) were identical for all docking jobs and are summarized in Table 5 (Supporting Information).

After docking, the 100 solutions were clustered in groups with rms deviations less than 1.0 Å. The clusters were ranked by the lowest energy representative of each cluster. The docking experiments were performed on an Octane R12000, and the average CPU time for each compound was 3 h.

Energy Refinement of the CDK2/Ligand Complexes. The CDK2/**1a** complex obtained from the docking experiments was gradually refined in AMBER using a cutoff of 10.0 Å. The receptor structure was modified to include missing amino acids as described above. The initial complex was refined by progressively minimizing its potential energy. The optimizations were carried out in a continuum medium of relative permittivitty $\epsilon = 4r_{ij}$ for imitating the solvent environment. The resulting complex was considered to be the initial structure for the molecular dynamics simulation in water.

Molecular Dynamics in Water. The system was placed into a 20 Å radius spherical cap of 328 TIP3P water molecules centered on the center of mass of the bound ligand. The initial complex was refined by progressively minimizing its potential energy. Unrestrained 1000 ps MD simulations at 298 K and 1 atm were then run for the complex using the SANDER module in AMBER. SHAKE[42] was applied to all bonds involving hydrogens, and an integration step of 2 fs was used throughout. The simulation protocol involved a series of progressive energy minimizations followed by a 10 ps heating phase and 10 ps equilibration period before data collection. System coordinates were saved every 2 ps for further analysis.

Analysis of the MD Trajectories. Three-dimensional structures and trajectories were visually inspected using the computer graphics program SYBYL.[31] Root-mean-square (rms) deviations form the initial structures, and interatomic distances were monitored using CARNAL.[40] An average structure from the last 500 ps of the MD simulations in water was refined by means of steepest-descent energy minimizations, and the resulting complex was used for the energy analysis using ANAL.

Acknowledgment. We thank Carlos Pérez (Lilly S. A., Spain) for his help with AutoDock. This work was supported by the Dirección General de Estudios Superiores (Grant No. PB98-0055), CYTED, and the Universidad San Pablo-CEU (Grant No. 5-99/01). M.C. thanks Fundación Ramón Areces for financial support. We thank the CIEMAT (Spain) for computer time and facilities. The kinase assays were supported by the Ministère de la Recherche/INSERM/CNRS "Molécules et Cibles Thérapeutiques" Program and a grant from the EEC (FP6-2002-Life Sciences and Health, PROKINASE Research Project) (L.M.).

Supporting Information Available: Experimental details of compounds reported, AMBER parameters and partial atomic charges for compound **1a** (Tables 3 and 4), docking parameters (Table 5), and microanalysis data for evaluated compounds. This material is available free of charge via the Internet at http://pubs.acs.org.

References

(1) Knockaert, M.; Greengard, P.; Meijer, L. Pharmacological Inhibitors of Cyclin-Dependent Kinases. *Trends Biochem. Sci.* **2002**, *23*, 417−425.
(2) Malumbre, M.; Barbacid, M. To Cycle or Not To Cycle: A Critical Decision in Cancer. *Nat. Rev. Cancer* **2001**, *1*, 222−231.
(3) Huwe, A.; Mazitschek, R.; Giannis, A. Small Molecules as Inhibitors of Cyclin-Dependent Kinases. *Angew. Chem., Int. Ed.* **2003**, *42*, 2122−2138.
(4) Sielecki, T. M.; Boylan, J. F.; Benfield, P. A.; Trainor, G. L. Cyclin Dependent Kinase Inhibitors: Useful Targets in Cell Cycle Regulation. *J. Med. Chem.* **2000**, *43*, 1−18.
(5) Senderowicz, A. M.; Headlee, D.; Stinson, S. F.; Lush, R. M.; Kalil, N.; Villalba, L.; Hill, K.; Steinberg, S. M.; Figg, W. D.; Tompkins, A.; Arbuck, S. G.; Sausville, E. A. Phase I Trial of Continuous Infusion Flavopiridol, a Novel Cyclin-Dependent Kinase Inhibitor, in Patients with Refractory Neoplasms. *J. Clin. Oncol.* **1998**, *16*, 2986−2999.
(6) Sedlacek, H. H.; Czech, J.; Naik, R.; Kaur, G.; Worland, P.; Losiewicz, M.; Parker, B.; Carlson, B.; Smith, A.; Senderowicz, A.; Sausville, E. Flavopiridol (L86-8275, NSC-649890), a New Kinase Inhibitor for Tumor Therapy. *Int. J. Oncol.* **1996**, *9*, 1143−1168.
(7) Akinaga, S.; Sugiyama, K.; Akiyama, T. UCN-01 (7-Hydroxystaurosporine) and Other Indolocarbazole Compounds: A New Generation of Anti-Cancer Agents for the New Century? *Anti-Cancer Drug Des.* **2000**, *15*, 43−52.
(8) Witherington, J.; Bordas, V.; Garland, S. L.; Hickey, D. M. B.; Ife, R. J.; Liddle, J.; Saunders: M.; Smith, D. G.; Ward, R. W. 5-Aryl-pyrazolo[3,4-*b*]pyridines: Potent Inhibitors of Glycogen Synthase Kinase-3 (GSK-3). *Bioorg. Med. Chem. Lett.* **2003**, *13*, 1577−1580.

(9) Meijer, L.; Frajolet, M.; Greengard, P. Pharmacological inhibitors of glycogen synthase kinase-3. *Trends Pharmacol. Sci*. **2004**, *25*, 471−480.
(10) Buehler, C. A.; Smith, H. A.; Glenn, D. M.; Nayak, K. V. Physiologically Active Compounds. II. Hydrochlorides of Aminoesters of Substituted Benzilic and Glycolic Acids. *J. Org. Chem.* **1958**, *23*, 1432−1437.
(11) Chattaway, F. D.; Coulson, E. A. The Preparation of 4,4′-Dinitrobenzil. *J. Chem. Soc.* **1928**, 1361−1364.
(12) Trisler, J. C.; Frye, J. L. Reaction of Benzil with Cyanide Ion in Dimethyl Sulfoxide. *J. Org. Chem.* **1965**, *30*, 306−307.
(13) Middleton, W. J.; Bingham, E. M. α,α-Difluoroarylacetic Acids: Preparation from (Diethylamino)sulfur Trifluoride and α-Oxoarylacetates. *J. Org. Chem.* **1980**, *45*, 2883−2887.
(14) Kamal El-Dean, A. M.; Radwan, S. M.; Abdel Moneam, M. I. Synthesis and Reactivity of Some Pyridazine Derivatives. *Afinidad* **1996**, *53*, 387−391.
(15) Borgne, A.; Meijer, L. Sequential dephosphorylation of $p34^{cdc2}$ on Thr-14 and Tyr-15 at the prophase/metaphase transition. *J. Biol. Chem.* **1996**, *271*, 27847−27854.
(16) Matsumoto, H.; Kaneko, C.; Yamada, K.; Takeuchi, T.; Mori, T.; Mizuno, Y. A Convenient Synthesis of 9-(2-Hydroxyethoxymethyl)guanine (Acyclovir) and Related Compounds. *Chem. Pharm. Bull.* **1988**, *36*, 1153−1157.
(17) Sims, P. A.; Wong, C. F.; McCammon, J. A. A Computational Model of Binding Thermodynamics: The Design of Cyclin-Dependent Kinase 2 Inhibitors. *J. Med. Chem.* **2003**, *46*, 3314−3325.
(18) McGrath, C. F.; Pattabiraman, N.; Kellogg, G. E.; Lemcke, T.; Kunick, C.; Sausville, E. A.; Zaharevitz, D. W.; Gussio, R. Homology Model of the CDK1/Cyclin B Complex. *J. Biomol. Struct. Dyn.* **2005**, *22*, 493−502.
(19) Teague, S. J. Implications of Protein Flexibility for Drug Discovery. *Nat. Rev. Drug Discovery* **2003**, *2*, 527−541.
(20) Khalifa, F. A. Synthesis and Reactions of Some Pyridazine Derivatives. *Arch. Pharm.* **1990**, *323*, 883−885.
(21) Schmidt, P.; Eichenberger, K.; Wilhelm, M. Strukturanaloga der Natürlichen Purin-Derivate (Structure Analogues of Natural Purine Derivatives). *Angew. Chem.* **1961**, *73*, 15−22.
(22) Albright, J. D.; Howell, C. F. Renin Inhibitors. US005459131, 2000.
(23) Carter, K. N.; Hulse, J. E. Extensions of the Hydrazone and Beckmann Rearrangements. *J. Org. Chem.* **1982**, *47*, 2208−2210.
(24) Kitamura, T.; Kyotani, Y.; Ohkuchi, M.; Yasuoka, K.; Furuyama, T.; Koshi, T.; Yoshizaki, H.; Matsuda, T.; Shigyo, H. Preparation of Pyridazin-3-one Derivatives as Interleukin-1b Inhibitors. WO0050408, 2000.
(25) Green, J.; Swenson, L.; Ter, H. E.; Arnost, M. J. Inhibitors of GSK-3 and Crystal Structures of GSK-3 b Protein and Protein Complexes. IWO02088078, 2002.
(26) Schmidt, P.; Druey, J. Heilmittelchemische Studien in der Heterocyclischen Reihe. Pyridazine II. Eine neue Pyridazinsynthese (Chemical Studies of Heterocyclic Compounds. Pyridazine 2. A New Pyridazine Synthesis). *Helv. Chim. Acta* **1954**, *37*, 134−140.
(27) Ward, R. W.; Witherington, J. Pyrazolopyridazine Derivatives, Process for Preparation and Use for the Inhibition of GSK-3. WO03080616, 2003.
(28) Wermuth, C.-G.; Schlewer, G.; Bourguignon, J.-J.; Maghioros, G.; Bouchet, M.-J.; Moire, C.; Kan, J.-P.; Worms, P.; Biziere, K. 3-Aminopyridazine Derivatives with Atypical Antidepressant, Serotonergic, and Dopaminergic Activities. *J. Med. Chem.* **1989**, *32*, 528−537.
(29) Seada, M.; Fawzy, M. M.; Jahine, H.; Abd El-Megid, M.; Saad, R. R. Synthesis and Biological Activities of Some New Pyridazine Derivatives. *J. Chin. Chem. Soc.* **1989**, *36*, 241−249.
(30) Braña, M. F.; Añorbe, L.; Tarrasón, G.; Mitjans, F.; Piulats, J. Synthesis and Biological Evaluation of Novel Bisindolylmaleimides That Inhibit Vascular Endothelial Cell Proliferation. *Bioorg. Med. Chem.* **2001**, *11*, 2701−2703.
(31) SYBYL, version 6.7; Tripos Inc. (1699 South Hanley Road, St. Louis, MO 63144); http://www.tripos.com.
(32) Mohamadi, F.; Richards, N. G. J.; Guida, W. C.; Liskamp, R.; Lipton, M.; Caufield, C.; Chang, G.; Hendrickson, T.; Still, W. C. MacroModel. An Integrated Software System for Modeling Organic and Bioorganic Molecules Using Molecular Mechanics. *J. Comput. Chem.* **1990**, *11*, 440−467.
(33) Weiner, S. J.; Kollman, P. A.; Case, D. A.; Singh, U. C.; Ghio, C.; Alagona, G.; Profeta, S.; Weiner, P. A New Force Field for Molecular Mechanical Simulation of Nucleic Acids and Proteins. *J. Am. Chem.* Soc. **1984**, *106*, 765−784.
(34) Still, W. C.; Temczyk, A.; Hawely, R. C.; Hendrickson, T. Searching Conformation Space. *J. Am. Chem. Soc*. **1990**, *112*, 6127−6129.
(35) Goodman, J. M.; Still, W. C. An Unbounded Systematic Search of Conformational Space. *J. Comput. Chem.* **1991**, *12*, 1110−1117.
(36) Frisch, M. J.; Trucks, G. W.; Schlegel, H. B.; Scuseria, G. E.; Robb, M. A.; Cheeseman, J. R.; Zakrzewski, V. G.; Montgomery, J. A., Jr.; Stratmann, R. E.; Burant, J. C.; Dapprich, S.; Millam, J. M.; Daniels, A. D.; Kudin, K. N.; Strain, M. C.; Farkas, O.; Tomasi, J.; Barone, V.; Cossi, M.; Cammi, R.; Mennucci, B.; Pomelli, C.; Adamo, C.; Clifford, S.; Ochterski, J.; Petersson, G. A.; Ayala, P. Y.; Cui, Q.; Morokuma, K.; Malick, D. K.; Rabuck, A. D.; Raghavachari, K.; Foresman, J. B.; Cioslowski, J.; Ortiz, J. V.; Stefanov, B. B.; Liu, G.; Liashenko, A.; Piskorz, P.; Komaromi, I.; Gomperts, R.; Martin, R. L.; Fox, D. J.; Keith, T.; Al-Laham, M. A.; Peng, C. Y.; Nanayakkara, A.; Gonzalez, C.; Challacombe, M.; Gill, P. M. W.; Johnson, B. G.; Chen, W.; Wong, M. W.; Andres, J. L.; Head-Gordon, M.; Replogle, E. S.; Pople, J. A. *Gaussian 98*, revision A.7; Gaussian, Inc.: Pittsburgh, PA, 1998.
(37) Bayly, C. I.; Cieplack, P.; Kollman, P. A. A Well-Behaved Electrostatic Potential Basic Method Using Charge Restraints for Deriving Atomic-Charges. The RESP Model. *J. Phys. Chem.* **1993**, *97*, 10269−10280.
(38) Cornell, W. D.; Cieplack, P.; Bayly, C. I.; Gould, I. R.; Merz, K. M.; Ferguson, D. M.; Spellmeyer, D. C.; Fox, T.; Caldwell, J. W.; Kollman, P. A. A Second Generation Force Field for the Simulation of Proteins, Nucleic Acids, and Organic Molecules. *J. Am. Chem. Soc.* **1995**, *117*, 5179−5197.
(39) Berman, H. M.; Westbrook, J.; Feng, Z.; Gilliland, G.; Bhat, T. N.; Weissig, H.; Shindyalov, I. N.; Bourne, P. E. The Protein Data Bank. *Nucleic Acids Res.* **2000**, *28*, 235−242.
(40) Case, D. A.; Pearlman, D. A.; Caldwell, J. W.; Cheatham, T. E., III; Ross, W. S.; Simmerling, C. L.; Darden, T. A.; Merz, K. M.; Stanton, R. V.; Cheng, A. L.; Vicent, J. J.; Crowly, M.; Ferguson, D. M.; Radmer, R. J.; Seibel, G. L.; Singh, U. C.; Weiner, P. K.; Kollman, P. A. *AMBER*, version 5; University of California: San Francisco.
(41) Morris, G. M. Automated Docking Using Lamarckian Genetic Algorithm and Empirical Binding Free Energy Function. *J. Comput. Chem.* **1998**, *19*, 1639−1662.
(42) Ryckaert, J. P.; Ciccoti, G.; Berendsen, H. J. C. Numerical Integration of the Cartesian Equations of Motion of a System with Constraints: Molecular Dynamics of *n*-Alkanes. *J. Comput. Phys.* **1977**, *23*, 327−341.

JM058013G